

Igor Ruban,
Hennadii Khudov,
Vladyslav Khudov,
Oleksandr Makoveichuk,
Irina Khizhnyak,
Ihor Butko,
Andrii Hryzo,
Rostyslav Khudov,
Petro Mynko,
Oleksii Baranik

DEVELOPMENT OF AN OPTOELECTRONIC IMAGE SEGMENTATION METHOD FROM UNMANNED AERIAL VEHICLES BASED ON THE ANT COLONY OPTIMIZATION ALGORITHM UNDER THE INFLUENCE OF SALT- AND-PEPPER NOISE

The object of research is the process of segmenting an image from an unmanned aerial vehicle based on the ant algorithm under the influence of salt-and-pepper noise.

"Salt"-and-"pepper" noise occurs due to data transmission errors, failures of digital camera sensors or malfunctions during recording/reading of information. It is characterized by the random appearance of individual pixels in the image, the value of which is equal to the minimum ("pepper") or maximum ("salt") brightness level.

Unlike the known ones, the method of segmenting an optoelectronic image based on the ant algorithm provides image segmentation under the influence of salt-and-pepper noise and involves:

- initialization of initial parameters;
- calculation of the length of the path segment of agents;
- calculation of the attractiveness of the route for the agent;
- updating the pheromone concentration;
- calculation of the probability of transition of agents;
- calculation of the objective function;
- movement of agents;
- determination of the best route of agents.

Experimental studies have shown that the segmentation method based on the ant algorithm provides a reduction in segmentation errors of the first kind on average:

- in the absence of salt-and-pepper noise – 4%;
- at the intensity of salt-and-pepper noise $\sigma = 5-21\%$;
- at the intensity of salt-and-pepper noise $\sigma = 15-10\%$.

The segmentation method based on the ant algorithm provides a reduction in segmentation errors of the second kind on average:

- in the absence of salt-and-pepper noise – 3%;
- at the intensity of salt-and-pepper noise $\sigma = 5-15\%$;
- at the intensity of salt-and-pepper noise $\sigma = 15-6\%$.

The practical significance of the segmentation method based on the ant algorithm is to ensure high-quality image segmentation under the influence of salt-and-pepper noise.

Keywords: optoelectronic image, segmentation, ant colony optimization algorithm, salt-and-pepper noise.

Received: 28.08.2025

Received in revised form: 22.10.2025

Accepted: 24.11.2025

Published: 29.12.2025

© The Author(s) 2025

This is an open access article
under the Creative Commons CC BY license
<https://creativecommons.org/licenses/by/4.0/>

How to cite

Ruban, I., Khudov, H., Khudov, V., Makoveichuk, O., Khizhnyak, I., Butko, I., Hryzo, A., Khudov, R., Mynko, P., Baranik, O. (2025). Development of an optoelectronic image segmentation method from unmanned aerial vehicles based on the ant colony optimization algorithm under the influence of salt-and-pepper noise. *Technology Audit and Production Reserves*, 6 (2 (86)), 68–75. <https://doi.org/10.15587/2706-5448.2025.344562>

1. Introduction

The modern development of unmanned aerial vehicles (UAVs) opens up extremely wide opportunities for the collection, process-

ing and practical use of observation information. Modern UAVs are equipped with high-precision sensors (cameras, thermal imagers, laser scanners, etc.). UAVs are able to provide detailed observation and monitoring to solve diverse tasks [1]. For example, in agriculture, monitoring

information is used to determine the condition of the soil and the level of plant moisture. In environmental monitoring, UAVs allow to track changes in the environment and respond to emergencies in a timely manner. In the military sphere, UAVs are used for aerial reconnaissance. In mapping, high-precision digital maps and 3D terrain models are created using UAVs, etc. [2, 3].

One of the key stages of processing images obtained from UAVs is the segmentation process. Segmentation involves dividing the image into homogeneous areas or individual objects [4].

The quality of segmentation directly determines the accuracy and reliability of analytical results, which makes it a critically important stage in image processing systems obtained from UAVs [5].

The quality of segmentation deteriorates under the influence of various noises. The formation of noise is due to the action of a combination of hardware, software and external factors.

The main noises caused by optoelectronic surveillance equipment include [6, 7]:

- temperature noise (Johnson-Nyquist noise), which is caused by thermal fluctuations of electrons in the matrix, especially when operating in high or low temperature conditions;
- reading noise, which occurs during the digitization of an analog signal by a sensor and an analog-digital device, which causes random errors in brightness reproduction;
- dark current, which manifests itself even in the absence of lighting in the form of "graininess", distorting the image.

The main noises caused by information processing and transmission are [6, 7]:

- impulse noise (salt-and-pepper), which leads to the appearance of single black and white dots in the image;
- quantization noise, which is formed due to the limited bit depth of the signal.

Also, external conditions have a significant impact on the quality of images, such as [6, 7]:

- atmospheric interference – rain, fog, dust, smoke or air turbulence, etc.;
- electromagnetic interference.

In [8], the main types of noise that affect the quality of an optoelectronic image are given: Gaussian, speckle noise and salt-and-pepper noise, and the nature of their occurrence are considered. The main source of Gaussian noise is electronic fluctuations. Speckle noise affects the image, causing it to be grainy, which makes it difficult to distinguish small details. Salt-and-pepper noise causes the presence of single pixels of white or black color.

Thus, the analysis [8] showed that the appearance of these noises significantly complicates the task of processing optoelectronic images and requires improvement of their processing methods at each stage. In this case, special attention is paid to the pre-processing stage and the stage of segmentation of the optoelectronic image. In [9], the use of the modified Fuzzy C-Means (FCM) method is proposed for segmentation of optoelectronic images distorted by noise of various nature. The main advantage of [9] is the high quality of segmentation results compared to the classical fuzzy clustering algorithm FCM. The main disadvantage of [9] is the dependence on the parameters of the weight coefficients, which, in turn, requires their careful adjustment for a specific task.

In [10], it is proposed to use the power mean function in combination with a fuzzy membership function for segmentation. This allows to reduce the influence of noise. The method proposed in [10] shows good results in isolating objects of interest on the test image, even under the condition of a low signal-to-noise ratio. However, it is difficult to assess the quality of segmentation on real images obtained from UAVs due to the fact that segmentation was not performed on such images. Another disadvantage of [10] is the dependence of the quality of the segmentation result on the correct choice of the parameter in the power mean function. In [11], it is proposed to use the approach of dividing labels

into "clean" and "noisy" (clean label disentangling) with the subsequent generation of pseudo-labels and to use this approach when training neural networks. The advantage of [11] is good segmentation results compared to methods based on a similar label distribution strategy. The disadvantage of [11] is the direct dependence of the quality of the segmentation results on the correctness of the selection of "clean" labels in the image.

In [12], it is proposed to use an approach that combines the use of two methods when segmenting medical images. This is the method of automatically generated pseudo-labels, and the method of "competitive" learning taking into account weight loss functions. Experimental studies on an open dataset of medical images have shown that the method [12] provides high-quality segmentation. However, the method has been tested only on medical images. There is also a dependence of the method on the initial pseudo-labels. This limits its use to images from UAVs.

In [13], it is proposed to use a neural network for segmenting images distorted by noise of various origins. In this case, the neural network independently makes decisions regarding the structure of the image, separating the noise. The experimental studies presented in [13] prove the effectiveness of the proposed approach when segmenting images distorted by noise of various types. The main disadvantages of [13] are high computational costs and the dependence of the segmentation result on the choice of initial parameters of the method.

In [14], a hybrid method is proposed for segmenting images distorted by noise. The method is based on an impulse neural network and an algorithm based on whale behavior (improved whale optimization algorithm). The main advantage of [14] is the high quality of segmentation of images distorted by noise of various nature. The disadvantage of [14] is the high computational costs associated with the sequential operation of the algorithm and the neural network. Therefore, the method cannot be used in real-time image processing.

In [15], an ant algorithm is proposed for segmenting optoelectronic images distorted by additive Gaussian noise. The main advantage of [15] is the adaptability of the method and the ability to self-adjust. This ensures high quality of segmentation, even with a significant level of additive Gaussian noise. The main disadvantage of [15] is the dependence of the segmentation result on the choice of the parameters of the ant algorithm.

In [16], a segmentation method based on the ant algorithm is proposed for segmenting optoelectronic images from UAVs that are distorted by speckle noise. The main advantage of [16] is to reduce the negative impact of speckle noise and improve the quality of segmentation. The disadvantage of [16] is the same as in the previous work, namely the dependence of the segmentation results on the setting of the input parameters of the algorithm.

Thus, the experimental studies presented in [15, 16] show the prospects of using the ant algorithm for segmenting images from UAVs that are distorted by noise. Therefore, the article proposes a method for segmenting optoelectronic images from UAVs based on the ant algorithm under the influence of salt-and-pepper noise.

The object of research is the process of segmenting an image from a UAV based on the ant algorithm under the influence of salt-and-pepper noise.

The aim of research is to improve the quality of segmentation of UAV images under the influence of salt-and-pepper noise.

To achieve the aim, it is necessary to perform the following objectives:

1. Provide a brief description of salt-and-pepper noise in an image from an unmanned aerial vehicle.
2. Provide the main stages of the image segmentation method based on the ant algorithm.
3. Conduct experimental studies on image segmentation using the ant algorithm method under the influence of salt-and-pepper noise.

2. Materials and Methods

The following assumptions were made during the research:

- only the optoelectronic image is considered;
- the influence of salt-and-pepper noise is considered;
- the influence of other noises is not considered;
- the comparison was made with the well-known Sobel method.

The following research methods were used:

- digital image processing;
- the mathematical apparatus of matrix theory;
- system analysis;
- comparative analysis;
- probability theory and mathematical statistics;
- optimization theory;
- swarm intelligence;
- mathematical modeling.

The research methods were selected based on the formulated research tasks. The choice of such research methods is due to:

- matrix representation of the image;
- the random nature of salt-and-pepper noise;
- use of the ant algorithm;
- iterative image processing process (experimental studies);
- comparative analysis of the developed method with known segmentation methods.

In a brief description of salt-and-pepper noise in an image from an unmanned aerial vehicle, the following theoretical methods were used:

- digital image processing;
- system analysis;
- probability theory and mathematical statistics;
- mathematical apparatus of matrix theory.

In determining the main stages of the image segmentation method based on the ant algorithm, the following theoretical methods were used:

- probability theory and mathematical statistics;
- optimization theory;
- system analysis;
- swarm intelligence.

In conducting experimental studies on image segmentation, the following experimental methods were used:

- mathematical modeling;
- digital image processing;
- comparative analysis.

When conducting experimental research, the following was used:

- hardware: Dell laptop Intel® Core™ i7-8650U CPU@ 1.90 GHz;
- software: object-oriented programming language Python 3.11, programming language Matlab 7 with application program package.

3. Results and Discussion

3.1. Brief description of salt-and-pepper noise in an image from an unmanned aerial vehicle

One of the common types of impulse noise that significantly affects the quality of digital images is salt-and-pepper noise. It is characterized by the random appearance of individual pixels in the image, the value of which is equal to the minimum (black color – "pepper") or maximum (white color – "salt") brightness level. Such noise occurs due to data transmission errors, failures of digital camera sensors or malfunctions during recording/reading of information.

Formally, salt-and-pepper impulse noise can be described as a random change in the brightness of an image pixel $f(X)$, where $X = (x, y)$ – coordinates of pixels in the image, according to the expression

$$f'(X) = \begin{cases} L_{\min}, & \text{with probability } p/2; \\ L_{\max}, & \text{with probability } p/2; \\ f(X), & \text{with probability } 1-p. \end{cases} \quad (1)$$

where L_{\min} – minimum value of noise intensity; L_{\max} – maximum value of noise intensity; p – noise density, which determines the proportion of distorted pixels.

The main feature of this type of noise is its impulsive nature and localization. As a result, single white and black dots appear. This leads to significant distortion of visual information and complicates image segmentation.

In [17] it is noted that median filters and their modifications are used for filtering salt-and-pepper noise. However, in conditions of high density of impulsive noise, the efficiency of these methods is significantly reduced. This necessitates the use of more adaptive approaches, among which bioinspired algorithms occupy a special place. Such algorithms are able to provide increased resistance to impulsive distortions.

Analysis of modern scientific publications shows that methods, in particular methods of image segmentation based on ant algorithms, are effective under conditions of influence of various noises. The use of ant algorithms in image segmentation tasks opens up the possibility of achieving high adaptability, noise resistance and improved processing quality even under difficult conditions.

3.2. The main stages of the image segmentation method based on the ant algorithm

The classical ant algorithm [18] has already been adapted for image segmentation. Each stage of the algorithm is modified taking into account the specifics of working with pixels and their features, such as brightness, color, texture [19].

Fig. 1 shows a block diagram of the image segmentation algorithm based on the ant algorithm (ACO).

This algorithm includes the following stages [19]:

1. Initialization of initial parameters:
 - the input image is denoted as $f(X)$;
 - the initial level of pheromone on all paths – F_0 ;
 - the pheromone evaporation coefficient – ρ ;
 - the coefficient α , which determines the influence of the pheromone on the choice of the route;
 - the coefficient β , which regulates the degree of "greed" when switching between nodes.
2. Initial arrangement of agents in the image.

In the first iteration of the ant algorithm, all agents are randomly placed on the pixels of the input image

$$X_{ii} = \text{rand}(f(X)), \quad (2)$$

where $X_{ij} = (x_{ij}, y_{ij})$ – the coordinates of the agent at the starting step; rand – the uniform random distribution function.

The number of agents is taken equal to the number of pixels of the analyzed image. Such initialization is performed only once, during the first iteration of the algorithm.

3. Calculation of the length of the path segment of the agents.

To determine the length of the route, the difference in brightness between neighboring pixels is taken into account, which is given by the expression

$$D_i^m(t) = |\Delta x_i^m(t)| + |\Delta y_i^m(t)| + k |\Delta f_i^m(t)|, \quad (3)$$

where m – the agent index; j – the algorithm iteration number; i – the image pixel; $|\Delta x_i^m(j)|$, $|\Delta y_i^m(j)|$ – the agent displacement along the x and y coordinate axes; k – coefficient that normalizes the differences in brightness (taking into account the scale, units of measurement, etc.); $|\Delta f_i^m(j)|$ – the difference in pixel brightness, which is determined by the formula

$$|\Delta f_i^m(j)| = |f(x_i^m(j), y_i^m(j)) - f(x_{i-1}^m(j), y_{i-1}^m(j))|. \quad (4)$$

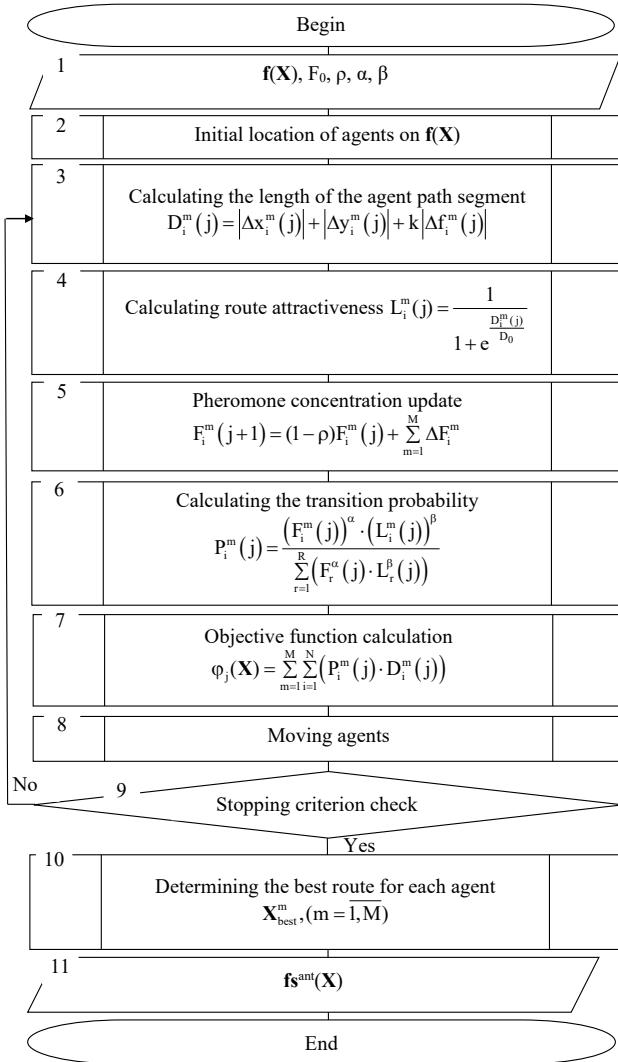


Fig. 1. Block diagram of the image segmentation algorithm based on the ant algorithm (ACO)

4. Calculation of the attractiveness of the route for the agent.

At each turning point of the movement, the "usefulness" of the selected route section is estimated by the ratios:

$$L_i^m(j) = \frac{1}{D_i^m(j)}, \quad (5)$$

$$L_i^m(j) = \frac{1}{1 + \frac{D_i^m(j)}{D_0}}, \quad (6)$$

$$L_i^m(j) = \frac{1}{1 + e^{\frac{D_i^m(j)}{D_0}}}, \quad (7)$$

where D_0 – a coefficient that scales the dependence on the image characteristics.

5. Updating the pheromone concentration.

At the initial step of the algorithm, the pheromone level for all sections of the route is considered the same and equal to the value F_0 . Subsequently, after each iteration, the amount of pheromone is adjusted according to the formula

$$F_i^m(j+1) = (1 - \rho)F_i^m(j) + \sum_{m=1}^M \Delta F_i^m, \quad (8)$$

where $\rho \in [0, 1]$ – the evaporation coefficient; ΔF_i^m – the additional contribution of pheromone after the agent passes through this section.

6. Calculation of the transition probability.

The choice of the next point of the agent's movement is determined by the rule

$$P_i^m(j) = \frac{(F_i^m(j))^\alpha \cdot (L_i^m(j))^\beta}{\sum_{r=1}^R (F_r^m(j) \cdot L_r^m(j))}, \quad (9)$$

where R – the number of possible turning points; $F_i^m(j)$ – the local concentration of pheromone at the selected point.

7. Calculation of the objective function.

To assess the quality of the route, the functional

$$\varphi_j(X) = \sum_{m=1}^M \sum_{i=1}^N (P_i^m(j) \cdot D_i^m(j)), \quad (10)$$

where N – the dimension of the input image.

8. Agent movement:

Each agent starts its path from the starting point, passes a sequence of intermediate nodes (selected according to the rule (9)) and ends its movement in the final position.

The optimal route is defined as one that minimizes the objective function (10). This principle fully corresponds to the methodology of swarm intelligence. In this case, the four-connectedness of pixels is taken into account, which is described by the relation

$$|\Delta x_i^m(j)| + |\Delta y_i^m(j)| = 1, \quad (11)$$

and then the objective function takes the form

$$\varphi_j(X) = \sum_{m=1}^M \sum_{i=1}^N \left(P_i^m(j) \cdot \left(1 + k \left| f(x_i^m(j), y_i^m(j)) - f(x_{i-1}^m(j), y_{i-1}^m(j)) \right| \right) \right), \quad (12)$$

and the optimization problem taking into account (12) is written as

$$\varphi_j(X) = \sum_{m=1}^M \sum_{i=1}^N \left(P_i^m(j) \cdot \left(1 + k \left| f(x_i^m(j), y_i^m(j)) - f(x_{i-1}^m(j), y_{i-1}^m(j)) \right| \right) \right) \rightarrow \min. \quad (13)$$

The trajectories where the most pheromone accumulates become dominant; less promising paths eventually lose their attractiveness due to evaporation.

9. Checking the stopping criterion:

If the termination condition is met, the algorithm proceeds to the next stage. If not, the calculation is repeated from Step 3.

10. Determining the best route:

For each agent, the optimal trajectory is calculated according to

$$X_{best}^m, \quad (m=1, M). \quad (14)$$

11. Formation of the final segmented image:

The output is a segmented image that corresponds to the optimal solution found by the ant colony.

3.3. Image segmentation under salt-and-pepper noise

To verify the operation of the segmentation method based on the ant algorithm under salt-and-pepper noise, experimental studies were conducted. The original image for segmentation is shown in Fig. 2 [16, 20].



Fig. 2. Initial image for experimental study [16, 20]

This is an optoelectronic image from the DJI Mavic 3 Pro (DJI RC) UAV (China) [16, 20]. Characteristics of the onboard optoelectronic equipment:

- wide-angle camera Complementary Metal-Oxide-Semiconductor (CMOS) Hasselblad, 20 MP;
- RAW image format;
- shooting speed 5.1 K/50 frames per second.

When conducting the experiment, by analogy with [16], the following assumptions were made:

- the optoelectronic image has a Red-Green-Blue (RGB) color space;
- objects of interest are a vehicle and a trailer;
- salt-and-pepper noise is considered;
- the influence of other distorting factors is not considered;
- hardware: Dell laptop Intel® Core™ i7-8650U CPU@ 1.90 GHz;
- software: object-oriented programming language Python 3.11, programming language Matlab 7 with application software package.

Fig. 3 shows the superimposition of salt-and-pepper noise with intensity $\sigma = 5$ on the original image (Fig. 2). Fig. 4 shows the superimposition of salt-and-pepper noise with intensity $\sigma = 15$ on the original image (Fig. 2).



Fig. 3. Original image (Fig. 2) with salt-and-pepper noise ($\sigma = 5$)



Fig. 4. Original image (Fig. 2) with salt-and-pepper noise ($\sigma = 15$)

Fig. 5–7 show segmented images (using the ant algorithm) at different values of salt-and-pepper noise intensity, namely:

- Fig. 5 – without noise influence $\sigma = 0$;
- Fig. 6 – at noise intensity $\sigma = 5$;
- Fig. 7 – at noise intensity $\sigma = 15$.



Fig. 5. Segmented original image (Fig. 2) without noise influence salt-and-pepper ($\sigma = 0$)

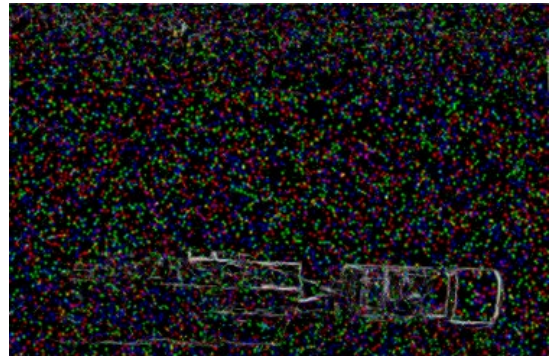


Fig. 6. Segmented original image (Fig. 2) at noise intensity ($\sigma = 5$)

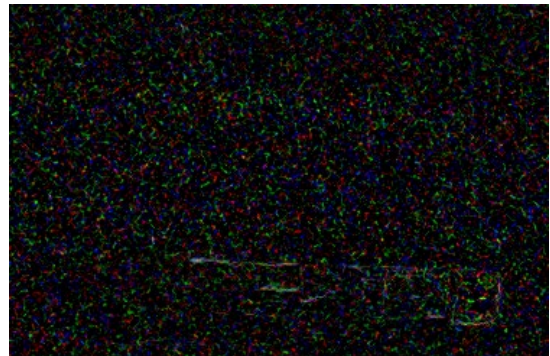


Fig. 7. Segmented original image (Fig. 2) at noise intensity ($\sigma = 15$)

Fig. 8–10 show segmented images (by the well-known Sobel method) at different values of noise intensity salt-and-pepper, namely:

- Fig. 8 – without noise $\sigma = 0$;
- Fig. 9 – at noise intensity $\sigma = 5$;
- Fig. 10 – at noise intensity $\sigma = 15$.

For comparative analysis, Fig. 8–10 show the results of segmentation of the same images by the method based on the Sobel operator [10]. In particular, Fig. 8 illustrates the result for an image without noise, Fig. 9 at noise level $\sigma = 5$, and Fig. 10 at noise level $\sigma = 15$.

Visual analysis of Fig. 5–10 indicates a better quality of segmented images using the method based on the ant algorithm (Fig. 5–7).

Let's calculate the segmentation errors of the first and second kind. Let's calculate the errors using the expressions (15) (first kind premise), (16) (second kind error) [16]:

$$\alpha_1 = \frac{S_1(f_s(X))}{S_2(f(X))}, \quad (15)$$

$$\beta_2 = 1 - \frac{S_3(f_s(X))}{S_4(f(X))}, \quad (16)$$

where $f_s(X)$ – the segmented image; $S_1(f_s(X))$ – the number of background pixels incorrectly attributed to objects of interest in the image $f_s(X)$; $S_2(f(X))$ – the number of background pixels in the image $f(X)$; $S_3(f_s(X))$ – the number of correctly segmented pixels of objects of interest in the image $f_s(X)$; $S_4(f(X))$ – the number of pixels of objects of interest in the image $f(X)$.



Fig. 8. Segmented original image (Fig. 2) by the well-known Sobel method without noise ($\sigma = 0$)

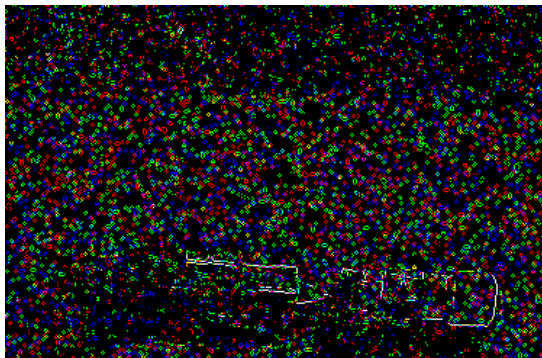


Fig. 9. Segmented by the well-known Sobel method the original image (Fig. 2) at noise intensity ($\sigma = 5$)

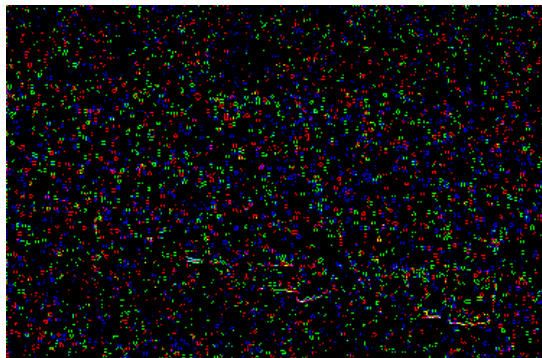


Fig. 10. Segmented by the well-known Sobel method the original image (Fig. 2) at noise intensity ($\sigma = 15$)

Table 1 and Table 2 show the values of segmentation errors of the first (α_1) and second (β_2) kind. Different values of salt-and-pepper noise intensity are taken into account.

Table 1

Segmentation error of the first kind (α_1)

Name of the segmentation method	Segmentation error of the first kind (α_1), %		
	Salt-and-pepper noise intensity (σ)		
	$\sigma = 0$	$\sigma = 5$	$\sigma = 15$
Sobel operator-based method	27.6	76.9	96.8
Ant algorithm-based method	23.9	55.5	86.6

Table 2

Segmentation error of the second kind (β_2)

Name of the segmentation method	Segmentation error of the second kind (β_2), %		
	Salt-and-pepper noise intensity (σ)		
	$\sigma = 0$	$\sigma = 5$	$\sigma = 15$
Sobel operator-based method	25.3	62.8	91.2
Ant algorithm-based method	22.5	47.3	85.6

From the analysis of Table 1 and Table 2 it is clear that the use of the ant algorithm in image segmentation provides a reduction in segmentation errors of the first kind on average:

- in the absence of salt-and-pepper noise – 4%;
- with the intensity of salt-and-pepper noise $\sigma = 5$ –21%;
- with the intensity of salt-and-pepper noise $\sigma = 15$ –10%.

From the analysis of Table 1 and Table 2 it is clear that the use of the ant algorithm in image segmentation provides a reduction in segmentation errors of the second kind on average:

- in the absence of salt-and-pepper noise – 3%;
- with the intensity of salt-and-pepper noise $\sigma = 5$ –15%;
- with the intensity of salt-and-pepper noise $\sigma = 15$ –6%.

The practical value of the segmentation method based on the ant algorithm is to ensure high-quality image segmentation under the influence of salt-and-pepper noise.

The following limits of application of the obtained results were adopted when conducting the research:

- application only for optoelectronic images;
- for quantitative calculations, only segmentation errors of the first and second kind were used.

The limitations of research are:

- quantitative indicators of segmentation quality are relevant only when the image is affected by only salt-and-pepper noise;
- it is necessary to first provide rotation compensation and scale change of the original optoelectronic image;
- it is not determined (on board or on the ground) where the segmentation of the optoelectronic image should be performed.

The prospects for further research are: calculation of other indicators of segmentation quality of optoelectronic images.

4. Conclusions

1. It was established that salt-and-pepper noise occurs as a result of data transmission errors, failures of digital camera sensors or malfunctions during recording/reading of information. It is characterized by the random appearance of individual pixels in the image, the value of which is equal to the minimum ("pepper") or maximum ("salt") brightness level.

2. Unlike the known ones, the main stages of the UAV image segmentation method based on the ant algorithm are:

- initialization of initial parameters;
- calculation of the length of the agent path segment;
- calculation of the attractiveness of the route for the agent;
- updating the pheromone concentration;

- calculation of the probability of agent transition;
- calculation of the objective function;
- movement of agents;
- determination of the best route for agents.

3. Experimental studies have been conducted on image segmentation under conditions of salt-and-pepper noise based on the ant algorithm under conditions of salt-and-pepper noise. It has been established that the segmentation method based on the ant algorithm provides a reduction in segmentation errors of the first kind on average:

- in the absence of salt-and-pepper noise – 4%;
- at the salt-and-pepper noise intensity $\sigma = 5-21\%$;
- at the salt-and-pepper noise intensity $\sigma = 15-10\%$.

It was found that the segmentation method based on the ant algorithm provides a reduction in segmentation errors of the second kind on average:

- in the absence of salt-and-pepper noise – 3%;
- at the salt-and-pepper noise intensity $\sigma = 5-15\%$;
- at the salt-and-pepper noise intensity $\sigma = 15-6\%$.

The practical significance of the segmentation method based on the ant algorithm is to ensure high-quality image segmentation under the influence of salt-and-pepper noise.

Conflict of interest

The authors declare that they have no conflict of interest regarding this research, including financial, personal, authorship or other, that could affect the research and its results presented in this article.

Financing

The research was conducted with grant support from the National Research Foundation of Ukraine within the framework of the competition "Science for Strengthening the Defense Capability of Ukraine", project "Information technology for automated segmentation of object images in FPV strike drone targeting systems based on swarm intelligence algorithms", registration number 2023.04/0153.

Data availability

Data will be provided upon reasonable request.

Use of artificial intelligence

The authors used the GPT-5.1 "Thinking" artificial intelligence tool in the research. The artificial intelligence tool was used to search for sources using keywords and criteria entered by the authors in the "Introduction" section. This was done to conduct a qualitative analysis of known methods for segmenting images from UAVs.

The authors checked the results provided by the artificial intelligence tool by analyzing the sources by their DOI (DOIs of all sources are indicated in the list of sources). The use of artificial intelligence contributed to increasing the completeness and quality of the analysis of literary sources.

Authors' contributions

Igor Ruban: general idea, definition of terminology, conducting a formal analysis of the choice of research methods, conducting an experimental study on image segmentation under the influence of salt-and-pepper noise; **Hennadii Khudov:** general idea, management activities for annotation (creation of metadata), data cleaning and support of research data (including software code for conducting an experimental study on image segmentation under conditions of salt-and-pepper noise, data interpretation, supervision and leadership responsibility

for planning and execution of research activities, including mentoring outside the core team, obtaining financial support for the project, which led to this publication; **Vladyslav Khudov:** general idea, formulation of the goal and main objectives of research, definition of terminology, development and creation of research methodology, definition of terminology for conducting the research, programming, software development, testing of existing code components, definition of research methods, preparation, creation and presentation of the published work, including writing the initial version; **Oleksandr Makoveichuk:** development or design of the methodology; creation of models, programming, implementation of computer code, testing of existing code components; **Irina Khizhnyak:** verification, as part of the activity or separately, of the overall reproducibility of experiments and other research results, application of statistical, mathematical, computational or other formal methods to analyze or synthesize research data, obtaining financial support for the project that led to this publication, responsibility for managing and coordinating the planning and execution of research activities; **Ihor Butko:** preparation, creation and/or presentation of the published work, including writing the initial version (including substantial translation), preparation, creation and/or presentation of the published work by members of the original research team, including critical review, comments or editing – including stages prior to publication; **Andrii Hryzo:** conducting the research process, including conducting experiments or collecting data, providing research materials, equipment, computing resources and other analytical tools; **Rostyslav Khudov:** general idea, formulation of the purpose and main objectives of research, development and creation of the research methodology, definition of terminology for conducting the research, programming, software development, testing of existing code components, definition of research methods, preparation, creation and presentation published work, including writing the initial draft; preparation, creation and presentation of published work, including presenting data; **Petro Mynko:** conducting the research and investigation process, including conducting experiments or collecting data/evidence; **Oleksii Baranik:** preparation, creation and/or presentation of published work, including visualizing/presenting data.

References

1. Zhang, Z., Zhu, L. (2023). A Review on Unmanned Aerial Vehicle Remote Sensing: Platforms, Sensors, Data Processing Methods, and Applications. *Drones*, 7 (6), 398. <https://doi.org/10.3390/drones7060398>
2. Nersisyan, G. (2024). Upcoming Military Applications of Unmanned Aerial Vehicles with Digital Cameras and Other Sensors. *Journal of Student Research*, 13 (1). <https://doi.org/10.47611/jsrv13i1.2378>
3. Bazrafkan, A., Igathinathane, C., Bandillo, N., Flores, P. (2025). Optimizing integration techniques for UAS and satellite image data in precision agriculture – a review. *Frontiers in Remote Sensing*, 6. <https://doi.org/10.3389/frsen.2025.1622884>
4. Bovik, A. C. (2010). *Handbook of Image and Video Processing*. Massachusetts: Academic Press, 1384. Available at: https://books.google.com.ua/books/about/Handbook_of_Image_and_Video_Processing.html?id=UM_GCfJe88sC&redir_esc=y
5. Bishop, C. M. (2016). *Pattern Recognition and Machine Learning (Information Science and Statistics)*. Springer, 778. Available at: https://books.google.com.ua/books/about/Pattern_Recognition_and_Machine_Learning.html?hl=ru&id=kOXDTAEACAAJ&redir_esc=y
6. Khudov, H., Ruban, I., Makoveichuk, O., Stepanenko, Y., Khizhnyak, I., Glukhov, S. et al. (2021). Improved Imaging Model in the Presence of Multiplicative Spatially Extended Cloaking Interference. *International Journal of Emerging Technology and Advanced Engineering*, 11 (11), 189–198. https://doi.org/10.46338/ijetae1121_22
7. Khudov, H., Makoveichuk, O., Misiuk, D., Butko, I., Khizhnyak, I., Shamsrai, N. (2021). The Visual Information Structures Formation Model for the Visual Information Systems Processing. *2021 IEEE 3rd International Conference on Advanced Trends in Information Theory (ATIT)*. Kyiv, 15–19. <https://doi.org/10.1109/atit54053.2021.9678806>
8. Babak, V., Zaporozhets, A., Kuts, Y., Fryz, M., Scherbak, L. (2025). *Noise signals: Modelling and Analyses*. Cham: Springer, 222. <https://doi.org/10.1007/978-3-031-71093-3>

9. Wang, C., Pedrycz, W., Li, Z., Zhou, M. (2021). Residual-driven Fuzzy C-Means Clustering for Image Segmentation. *IEEE/CAA Journal of Automatica Sinica*, 8 (4), 876–889. <https://doi.org/10.1109/jas.2020.1003420>
10. Rahman, A., Ali, H., Badshah, N., Zakarya, M., Hussain, H., Rahman, I. U. et al. (2022). Power Mean Based Image Segmentation in the Presence of Noise. <https://doi.org/10.21203/rs.3.rs-1204261/v1>
11. Wang, Z., Zhao, Z., Guo, E., Zhou, L. (2023). Clean Label Disentangling for Medical Image Segmentation with Noisy Labels. *arXiv:2311.16580v1*. <https://doi.org/10.48550/arXiv.2311.16580>
12. Wang, L., Guo, D., Wang, G., Zhang, S. (2021). Annotation-Efficient Learning for Medical Image Segmentation Based on Noisy Pseudo Labels and Adversarial Learning. *IEEE Transactions on Medical Imaging*, 40 (10), 2795–2807. <https://doi.org/10.1109/tmi.2020.3047807>
13. Benfenati, A., Catozzi, A., Franchini, G., Porta, F. (2026). Unsupervised noisy image segmentation using Deep Image Prior. *Mathematics and Computers in Simulation*, 239, 986–1003. <https://doi.org/10.1016/j.matcom.2025.07.052>
14. Zhang, X. (2023). Image denoising and segmentation model construction based on IWOA-PCNN. *Scientific Reports*, 13 (1). <https://doi.org/10.1038/s41598-023-47089-6>
15. Gadetska, S., Dubnitskiy, V., Kushneruk, Y., Ponochovnyi, Y., Khodyrev, A. (2025). Determination of parameter-limited estimates of extreme value distributions and modeling of conditions for their occurrence using STAT-GRAPHICS and MATLAB. *Advanced Information Systems*, 9 (3), 32–41. <https://doi.org/10.20998/2522-9052.2025.3.04>
16. Ruban, I., Khudov, H., Khudov, V., Makoveichuk, O., Khizhnyak, I., Shamrai, N. et al. (2025). Development of an image segmentation method from unmanned aerial vehicles based on the ant colony algorithm under the influence of speckle noise. *Technology Audit and Production Reserves*, 4 (2 (84)), 80–86. <https://doi.org/10.15587/2706-5448.2025.334993>
17. Gonzalez, R., Woods, R. E. (2002). *Digital Image Processing*. Prentice Hall. Available at: [https://uodiyala.edu.iq/uploads/PDF%20ELIBRARY%20UODIYALA/EL31/\(%20DSP%20Book\)%20-%20Gonzalez%20e%20Woods%20-%20Digital%20Image%20Processing%20\(2nd%20ed\)%20-%20Prentice%20Hall%202002%20\(the%20only\).pdf](https://uodiyala.edu.iq/uploads/PDF%20ELIBRARY%20UODIYALA/EL31/(%20DSP%20Book)%20-%20Gonzalez%20e%20Woods%20-%20Digital%20Image%20Processing%20(2nd%20ed)%20-%20Prentice%20Hall%202002%20(the%20only).pdf)
18. Dorigo, M., Stutzle, T. (2004). *Ant Colony Optimization*. Cambridge: MIT Press. <https://doi.org/10.7551/mitpress/1290.001.0001>
19. Khudov, H., Hridasov, I., Khizhnyak, I., Yuzova, I., Solomenenko, Y. (2024). Segmentation of image from a first-person-view unmanned aerial vehicle based on a simple ant algorithm. *Eastern-European Journal of Enterprise Technologies*, 4 (9 (130)), 44–55. <https://doi.org/10.15587/1729-4061.2024.310372>
20. Bezkoshtovni resursi BPLA. *PortalGIS.pro*. Available at: <https://portalgis.pro/bpla/bezkoshtovni-resursy-bpla>

Igor Ruban, Doctor of Technical Sciences, Professor, Rector, Kharkiv National University of Radio Electronics, Kharkiv, Ukraine, ORCID: <https://orcid.org/0000-0002-4738-3286>

Hennadii Khudov, Doctor of Technical Sciences, Professor, Head of Department of Radar Troops Tactic, Ivan Kozhedub Kharkiv National Air Force University, Kharkiv, Ukraine, e-mail: 2345kh_hg@ukr.net, ORCID: <https://orcid.org/0000-0002-3311-2848>

Vladyslav Khudov, PhD, Junior Researcher, Department of Information Technology Security, Kharkiv National University of Radio Electronics, Kharkiv, Ukraine, ORCID: <https://orcid.org/0000-0002-9863-4743>

Oleksandr Makoveichuk, Doctor of Technical Sciences, Associate Professor, Department of Computer Sciences and Software Engineering, Higher Education Institution "Academician Yuriy Bugay International Scientific and Technical University", Kyiv, Ukraine, ORCID: <https://orcid.org/0000-0003-4425-016X>

Irina Khizhnyak, Scientific and Methodological Department for Quality Assurance in Educational Activities and Higher Education, Ivan Kozhedub Kharkiv National Air Force University, Kharkiv, Ukraine, ORCID: <https://orcid.org/0000-0003-3431-7631>

Ihor Butko, Doctor of Technical Sciences, Professor, Department of Computer Sciences and Software Engineering, Higher Education Institution "Academician Yuriy Bugay International Scientific and Technical University", Kyiv, Ukraine, ORCID: <https://orcid.org/0000-0002-2859-0351>

Andrii Hryzo, PhD, Associate Professor, Head of Research Laboratory, Department of Radar Troops Tactic, Ivan Kozhedub Kharkiv National Air Force University, Kharkiv, Ukraine, ORCID: <https://orcid.org/0000-0003-2483-5953>

Rostyslav Khudov, Department of Theoretical and Applied Informatics, V.N. Karazin Kharkiv National University, Kharkiv, Ukraine, ORCID: <https://orcid.org/0000-0002-6209-209X>

Petro Mynko, PhD, Associate Professor, Department of Higher Mathematics, National University of Radio Electronics, Kharkiv, Ukraine, ORCID: <https://orcid.org/0000-0002-2621-8900>

Oleksii Baranik, PhD, Associate Professor, Head of Department of Aviation Armament Complexes, Ivan Kozhedub Kharkiv National Air Force University, Kharkiv, Ukraine, ORCID: <https://orcid.org/0000-0002-1499-7943>

✉ Corresponding author